JOURNAL
OF THE AMERICAN CHEMICAL SOCIETY

VOLUME 97, NUMBER 19 SEPTEMBER 17, 1975

The Generalized Valence Bond Description of the Low-Lying States of Diazomethane[1]

Stephen P. Walch[2] and William A. Goddard III*

Contribution No. 5030 from the Arthur Amos Noyes Laboratory of Chemical Physics, California Institute of Technology, Pasadena, California 91125.
Received December 23, 1974

Abstract: We report ab initio generalized valence bond (GVB) and configuration interaction (CI) calculations (using a double-ζ basis) on the ground and low-lying excited states of diazomethane. We find that the ground state is more accurately described as a singlet biradical (somewhat as in ozone) than as a zwitterion. The calculated vertical excitation energies are 2.65 eV ($^3A_2$), 2.93 eV ($^1A_2$), 3.66 eV ($^3A_1$), and 5.90 eV (2^1A_1). The singlet excitation energies are in good agreement with the observed absorptions, broad continuum bands with peaks at 3.14 and 5.70 eV, leading hence to assignments of these transitions. Studies of the higher Rydberg states are also reported.

I. Introduction

The bond of the N_2 molecule is one of the strongest known bonds (D_0 = 9.756 eV) and is usually pictured as a triple bond involving two electrons in a σ bond and four electrons in two π bonds. This bond is so strong that atmospheric nitrogen is essentially unavailable to living organisms except for the fact that certain bacteria in the soil are able to convert N_2 into a more active form (no NN bonds). Indeed, an active and potentially important area of modern chemical research is the search for proper substrates and catalysts to first bond N_2 and then to break the NN bonds. Although several transition metal compounds have been found that bond N_2, it is generally not known whether the σ or π bonds are weakened by the bonding to the metal.[3]

As a first step into the investigation of such phenomena, we have considered the end-on bonding of N_2 to CH_2, that is the molecule diazomethane. The bonding in diazomethane is usually represented by the resonance structures

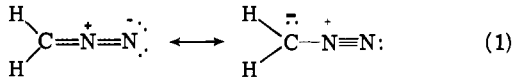

(1)

A peculiar fact about this system is that both of these structures involve charge separation. In fact, one cannot write a proper resonance structure for diazomethane without allowing charge separation.[4]

In this paper we present the results of generalized valence bond (GVB) calculations on the ground and excited states of diazomethane. This approach corresponds to a generalization of the valence bond method in which all orbitals are solved for self-consistently. The resulting wave function for diazomethane is basically that of a singlet biradical with strong bonding between the radical π orbitals on the C and

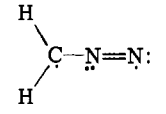

(2)

terminal N resulting from the interaction with the π pair on the central N.

The basic form of the wave function and other calculational details are discussed in section II. The wave function for the ground state of diazomethane is analyzed in section III and the excited states are discussed in section IV. The CI calculations are described in section V and some of the implications of these results for understanding the chemistry of diazomethane are presented in section VI.

II. The Wave Functions

A. The Perfect Pairing GVB Wave Functions. The generalized valence bond method (GVB) is described in some detail elsewhere.[5a] Here we will review some of the ideas important for presentation of our results.

The simple closed-shell Hartree–Fock (HF) wave function can be written as

$$\mathcal{A}\{[\varphi_1(1)\varphi_1(2)\alpha(1)\beta(2)][\varphi_2(3)\varphi_2(4)\alpha(3)\beta(4)]\ldots\} \quad (3)$$

where each HF molecular orbital φ_i is doubly occupied. [For simplicity we discuss the case of singlet states.] This restriction that the orbitals be doubly occupied leads to a number of difficulties in describing excited states and reac-

tions of molecules. To remove this restriction we replace the paired function

$$\varphi_i(1)\varphi_i(2) \tag{4}$$

in (3) by the pair function

$$\varphi_{ia}(1)\varphi_{ib}(2) + \varphi_{ib}(1)\varphi_{ia}(2) \tag{5}$$

leading then to

$$\mathcal{A}\{[\varphi_{1a}(1)\varphi_{1b}(2) + \varphi_{1b}(1)\varphi_{1a}(2)][\varphi 2_a(3)\varphi_{2b}(4) + \varphi_{2b}(3)\varphi_{2a}(4)]\ldots\chi\} \tag{6}$$

where

$$\chi = \alpha(1)\beta(2)\alpha(3)\beta(4)\ldots \tag{7}$$

[In the following, expressions such as (6) and (7) will have the electron numbers deleted, the orbitals being ordered with increasing electron number for each term.] The orbitals of (6) are then solved for self-consistently to obtain the GVB wave function.

In the GVB wave function no restrictions are made on the orbitals or on the spin function χ.[6] However, for computational convenience we have placed some restrictions on the orbitals of (6), namely, although the orbitals of a pair are allowed to have whatever overlap

$$\langle\varphi_{ia}|\varphi_{ib}\rangle$$

results from the variational principle, orbitals of different pairs are taken as orthogonal, that is

$$\begin{aligned}\langle\varphi_{ia}|\varphi_{jb}\rangle &= 0\\ \langle\varphi_{ia}|\varphi_{ja}\rangle &= 0\end{aligned} \tag{8}$$

if $i \neq j$. In addition, the spin function χ of (6) is restricted so that each pair is singlet coupled.[7] The resulting wave function is denoted as GVB-PP to indicate that these restrictions have been made (PP denotes "perfect pairing"). These restrictions are later relaxed and found to be of little consequence for the cases considered herein.

In solving for the GVB-PP wave function it is convenient to define natural orbitals, ϕ_{i1} and ϕ_{i2}, for each pair such that

$$C_1[\varphi_{i1}\varphi_{i1} - \lambda_i^2\varphi_{i2}\varphi_{i2}] = \phi_{ia}\phi_{ib} + \phi_{ib}\phi_{ia} \tag{9}$$

where

$$\begin{aligned}\varphi_{ia} &= N_i[\varphi_{i1} + \lambda\varphi_{i2}]\\ \varphi_{ib} &= N_i[\varphi_{i1} - \lambda_{i2}]\end{aligned} \tag{10}$$

The natural orbitals are orthogonal and lead to more convenient variational equations than do the GVB orbitals, φ_{ia} and φ_{ib}.

In the full GVB wave function every doubly occupied orbital of the HF wave function is replaced by two GVB orbitals. Although the GVB description of a pair leads to lower energies than the HF description, there are many cases where the same potential curves and excitation energies are obtained whether a particular pair is split or not. Examples are the 1s orbitals of first row atoms such as C and N and the 2s orbitals of O and F. Generally, it is only the bonding pairs that have to be described as GVB pairs (eq 5). As a result, we will often describe only a limited number of pairs in the GVB form (5), the others being described with doubly occupied orbitals, as in (4). Of course, *all* orbitals are solved for self-consistently. When only n pairs are split [that is, described as in (5)], we will use the notation GVB(n) or GVB(n/PP). For example, GVB(3) is quite sufficient for N_2 and GVB(6) is quite sufficient for diazomethane.

For triplet states we use GVB(n) to indicate that all but n pairs are doubly occupied. For perfect pairing a triplet state requires two orbitals to be antisymmetrically coupled

$$\phi_{ia}\phi_{ib} - \phi_{ib}\phi_{ia} \tag{5'}$$

rather than symmetrically coupled as in (5). Thus for a triplet state GVB(n/PP) implies $n - 1$ singlet pairs as (5) and one triplet pair as (5'). With this notation singlet and triplet states described to a comparable quality are denoted with the same n. (Note that for a triplet state GVB(1) is just the Hartree–Fock wave function.)

B. Calculational Details. All calculations presented here (ground and excited states) use the experimental geometry for the ground state:[8] R_{CH} = 1.077 Å, R_{CN} = 1.300 Å, R_{NN} = 1.139 Å, and ∠HCH = 126.1°. The axes are chosen so that the z direction coincides with the rotation axis and the yz plane is the molecular plane. With this convention, the B_1 and A_2 symmetries indicate orbitals antisymmetric with respect to the molecular plane (denoted collectively as $\bar{\pi}$) while the A_1 and B_2 symmetries indicate orbitals symmetric with respect to the molecular plane (denoted collectively as $\bar{\sigma}$). Note the bar in $\bar{\sigma}$ and $\bar{\pi}$; this is to distinguish these symmetries from the σ and π symmetries of diatomic molecules.

Three basis sets were used for the valence states. (1) MBS: a (7s,3p/3s) set of Gaussian primitive basis functions was contracted to a minimal basis set (2s,1p/1s) using a scale factor of 1.17 for the hydrogens.[9a] (2) DZ: the (9s,5p/4s) primitive set of Huzinaga was contracted to the double zeta basis (4s,2p/2s) of Dunning[9b] using a scale factor of 1.20 for the hydrogens. (3) DZR_x: the DZ basis was augmented with a single diffuse p_x primitive function on each N and C (ζ_N = 0.05153 and ζ_C = 0.03650).

For describing the Rydberg states we used the DZ basis and added on each N and C the following diffuse functions (all primitive Gaussians). (a) Two s functions chosen by scaling down the valence basis functions (orbital exponents: ξ_C = 0.04736, ξ_C' = 0.01460, ξ_N = 0.0650, and ξ_N' = 0.0198). (b) Two sets of p basis functions chosen in a similar manner (orbital exponents: ξ_C = 0.03654, ξ_C' = 0.01165, ξ_N = 0.05148, and ξ_N' = 0.01602).

The GVB(PP) calculations were carried out with the Bobrowicz–Wadt–Goddard program (GVBTWO)[10a] based on the Hunt, Hay, and Goddard[5b] fully self-consistent variational procedures. The CI calculations were carried out with the Caltech spin-eigenfunction CI program.[10b] The molecular integrals were calculated with a version of the POLYATOM integrals program and the properties were calculated using a version of the J. Moskowicz Gaussian properties program. The CI properties were obtained with a program written by T. H. Dunning, Jr., and S. P. Walch. The IVO calculations were carried out using a specialized version (W. R. Wadt) of the GVBTWO program.

III. The Ground State

A. Introduction. For the ground state of carbon the GVB wave function yields orbitals that can be schematically represented[5a,c] as

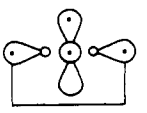

(11)

where

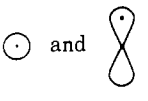

and (12)

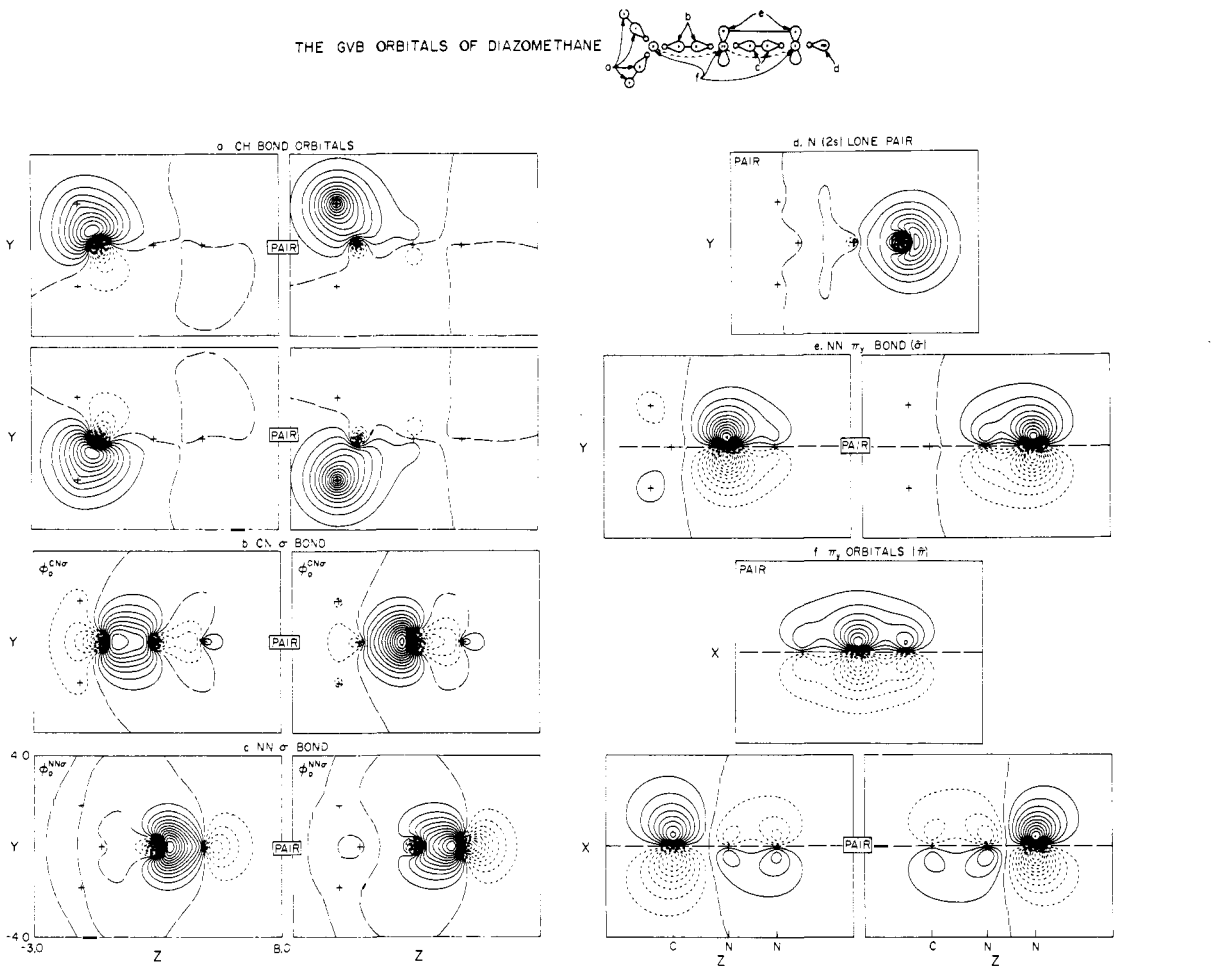

Figure 1. The GVB(6/PP) orbitals of the $X(^1A_1)$ state of diazomethane. The molecule is in the yz plane. Long dashes indicate zero amplitude. The contours represent constant amplitudes with a difference of 0.05 au between contours. The positions of the nuclei are denoted by +. The same conventions are used for all other plots (unless otherwise noted).

indicate singly occupied orbitals perpendicular and parallel to the paper, respectively, and

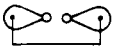

(13)

indicates the angularly correlated 2s pair. Studies of various carbon containing molecules[5] have shown that the geometries and ordering of states can be simply understood in terms of coupling the orbitals of the other atoms to the orbitals of (11). Thus, the ground state of C_2 is[5c] ($^1\Sigma_g^+$)

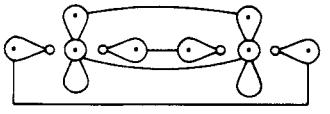

(14)

and the ground state of CO is[5d]

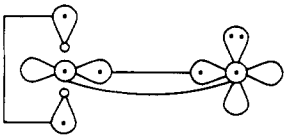

(15)

where the lines between singly occupied orbitals indicate bond (singlet coupled) pairs. The tetravalent character of carbon can thus be understood in terms of the four GVB orbitals of the ground state of carbon.[5]

For the ground state of the nitrogen atom (^4S), the presence of a singly occupied orbital in each direction restricts the angular correlation of the 2s pairs, leading to just three orbitals that can form bonding pairs (the 2s doubly occupied orbital is omitted).[11]

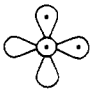

(16)

Thus, the trivalent character of nitrogen follows directly from (16). The $(2s)^2(2p)^3$ configuration of N also leads to ^2D and ^2P states and for the ^2P state there is a strong angular correlation effect just as in $C(^3P)$. The ^2P wave function is schematically represented as

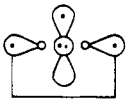

(17)

Starting with (17) for the central nitrogen atom, bringing up a $N(^4S)$ on the right [as in (16)] and the ground state ($^3B_1$) of methylene [as in (18)]

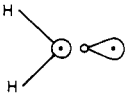

(18)

on the left leads to a description of diazomethane

Table I. Dipole Moment Breakdown for the X^1A_1 and 1^1A_2 states of H_2CNN[a]

State	Pair	Orbital contribution, au[c]	Occupation no.	Pair contribution, D
$X(^1A_1)$	N 2s	0.3973	0000	2.018
	NN σ	0.1426	1.994	0.7245
	NN σ^*	0.1571	0.0062	
	CN σ	0.1958	1.992	0.9858
	CN σ^*	−0.2221	0.0083	
	CH σ_l	−0.0733	1.987	−0.3744
	CH σ_l^*	−0.1393	0.0126	
	CH σ_r	−0.733	1.987	−0.3744
	CH σ_r^*	−0.1393	0.0126	
	NN π_y (b_2)	−0.2372	1.925	−1.1437
	NN π_y^* (b_2)	0.0839	0.0750	
	$1\pi_x$	0.1631	2.000	0.8287
	$2\pi_x$	−0.1366	1.884	−0.6821
	$3\pi_x$	−0.0971	0.116	
			Total =	1.9824 D
1^1A_2	N 2s	0.453	2.000	2.3012
	NN σ	0.0617	2.000	0.3134
	CN σ	0.163	1.991	0.8199
	CN σ^*	−0.196	0.0089	
	CH (a_1)	−0.234	2.000	−1.1887
	CH (b_2)[b]	−0.234	2.000	−1.1887
	$2b_2$	0.967	2.000	4.9124
	$3b_2$	−0.826	1.000	−2.0980
	$1\pi_x$	−0.319	1.952	−1.5979
	$1\pi_x^*$	−0.133	0.04798	
	$2\pi_x$	0.327	1.000	0.8306
			Total =	3.104 D

[a] The nuclear charge is partitioned in a manner consistent with (10) for the X^1A_1 state and consistent with (25) in the case of the 1^1A_2 state. [b] Since the $1b_2$, $2b_2$ orbitals are in the same shell, the energy and other properties are invariant to a nonsingular transformation among them. We have used this freedom to fix the orbital contribution for the CH (b_2) orbital to that for the CH (a_1) orbital. The value for the $2b_2$ orbital was then determined by requiring that the total dipole moment remain constant. [c] 1 au of dipole moment equals 2.54158 D.

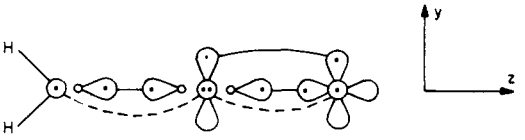

(19)

close to that found from the GVB calculations on H_2CNN.

B. The GVB Orbitals. The GVB orbitals of the ground state of diazomethane are shown in Figure 1. In describing these orbitals we will find it useful to discuss the contribution to the dipole moment for each pair and to compare with the value expected from the GVB model. To make this comparison we partition the nuclear contributions among the orbital pairs just as suggested by (19). [Thus the NN σ pair has associated with it one nuclear charge on each N.] The results are shown in Table I, where a positive dipole moment indicates extra electrons have moved toward the terminal N.

Of the four orbitals involved in the CN and NN σ bonds, two ($\phi_b^{CN\sigma}$ and $\phi_a^{NN\sigma}$) are concentrated on the nitrogen. These orbitals correspond to the lobe orbitals of (17) [the self-consistent orbitals of (17) are shown in Figure 2] and as expected are very similar to each other. Note that $\phi_a^{CN\sigma}$ is slightly delocalized onto the N whereas $\phi_b^{CN\sigma}$ is more atomic like; this is typical of a slightly ionic bond (toward the N) and indeed this pair contributes +0.986 D to the dipole moment. The $\phi_b^{NN\sigma}$ orbital in Figure 1c corresponds to the p_z orbital of (16) but delocalized slightly onto the central N. The NN pair contributes +0.724 D to the dipole moment indicating a slightly ionic bond toward the terminal N.

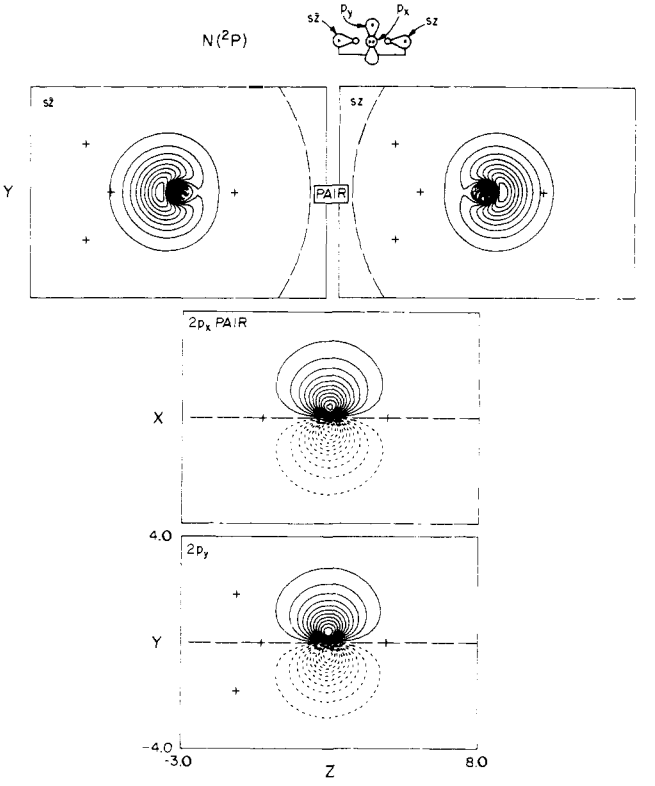

Figure 2. The GVB(1/PP) orbitals of the ^2P state of the N atom.

The orbital in Figure 1d is doubly occupied and corresponds to the 2s pair of N(^4S). As is typical of the 2s pairs of N, O, and F, it has shifted away from the bonding pairs. This effect derives essentially from the repulsive interaction between the 2s pairs and the bond pairs (arising from the Pauli principle). This pair contributes +2.018 D to the dipole moment, the dominant contribution.

The orbitals in Figure 1e correspond to a π_y bond between the nitrogens but in the plane of the molecule (that is, the π bond orbitals of N_2 are $\bar{\sigma}$ orbitals for H_2CNN). This π bond is quite similar to that of N_2. It is delocalized to the left, contributing −1.144 D to the dipole moment. This shift is probably in response to the shift in the σ orbitals to the right.

The orbitals corresponding to the two CH bonds (Figure 1a) correspond closely to the CH bond orbitals of CH_2[5c] and of H_2CO.[12] The total dipole moment contribution for a CH pair in CH_2N_2 is 1.577 D(H^-C^+) directed at an angle of 76.3° with the z axis as compared to the internuclear angle of 63.1°. However, only the z component contributes to the net dipole, leading to a contribution of −0.374 D per CH pair. The slight delocalization of the H like orbitals onto the near nitrogen probably explains the fact that the dipole contribution is not directed along the bond.

The remaining orbitals (Figure 1f) are $\bar{\pi}$ type (we will denote these as π_x) and exhibit some unusual characteristics. We find that this four-electron system is described by

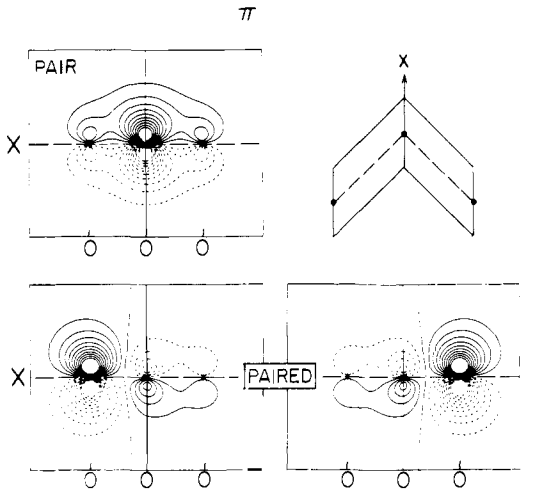

Figure 3. The GVB(3/PP) $\bar{\pi}$ orbitals of ozone.

one doubly occupied pair (denoted as ϕ_c) consisting of components localized mainly on the center nitrogen and a GVB pair consisting of components localized mainly on the carbon and on the end nitrogen (denoted as ϕ_l and ϕ_r, respectively),

$$(\phi_c)^2(\phi_l\phi_r + \phi_r\phi_l) \tag{20}$$

This four-electron π_x system in diazomethane bears a formal resemblance to the π^4 system of ozone.[5a] However, in the case of diazomethane the $\varphi_l\varphi_r$ GVB pair has a much higher overlap (S_{lr} = 0.60) than is the case in ozone (S_{lr} = 0.28). Thus, while ozone is represented as a biradical with weak coupling between the biradical orbitals (single–triplet separation of 1.4 eV), such a description is less appropriate to CH_2N_2. The singlet–triplet splitting here is 3.7 eV (vertical), which is comparable to the vertical singlet–triplet separation for a normal π bond (4.2 eV for ethylene, 3.5 eV for formaldehyde).

The $\bar{\pi}$ orbitals of the ground state of ozone are shown in Figure 3. A close comparison between these orbitals and the π_x orbitals of diazomethane provides some insight into the difference between the two systems. The reason for the moderate overlap of the $\varphi_l\varphi_r$ pair of ozone is that each component of the pair builds in a nodal plane in the region of the center O in order to remain orthogonal to the doubly occupied orbital. This results in a moderate amplitude for both φ_l and φ_r near the center O and a moderate overlap for the pair. However, in the case of diazomethane the doubly occupied orbital is asymmetric with the center of density shifted toward the end nitrogen. Thus the φ_l component of the GVB pair has its nodal plane shifted toward the right. This results in a moderate amplitude for this orbital in the vicinity of the end nitrogen, where the φ_r orbital has its maximum. At the same time the φ_r orbital becomes more antibonding due to the higher overlap with the φ_c orbital, causing increased density near the C where the φ_l orbital is maximum. The overall result is a much higher overlap for the GVB π_x pair than occurs in ozone.

The ϕ_c pair leads to a contribution of +0.829 D to the dipole moment (as expected from its delocalization onto the terminal N). However, the other pair contributes −0.682 D to the dipole moment leading to a net contribution of +0.147 D due to the π_x orbitals.

Summarizing the trends in the dipole moments, we find that the CNN σ orbitals all shift to the right (a net shift of +3.728 D), the π_y and CH orbitals shift in the opposite direction (−1.892 D), while the $\bar{\pi}$ orbitals lead to little net shift (0.147 D). Thus, the large positive dipole moment of the ground state is dominated by effects in the $\bar{\sigma}$ system. The most important single contribution to the dipole moment arises from the N(2s) pair. This effect is a result of the hybridization of the N(2s) pair away from the bonding orbitals (an effect arising from the Pauli principle and which is not reflected in the Mulliken population analysis). Additionally, the CH and CN σ bonds as a whole give a net positive contribution as expected from electronegativity. However, the NN $\pi_y(\bar{\sigma})$ pair contributes negatively. (This complicated effect derives from the flow of change onto the end nitrogen in the $\bar{\pi}_x$ system which was in turn a response to the polarity of the CN bonding pair.) This result serves to emphasize the point that electronegativity differences alone are not sufficient for predicting dipole moments (e.g., CO,[13] NO,[14,15] and CF[14] all have "reversed" dipole moments).

Most of the small discrepancy (~0.3 D) of the CI dipole moment with experiment is probably due to a need for d polarization functions not included in our DZ basis.

C. Mulliken Populations. Since Hartree–Fock and MO wave functions are often analyzed in terms of Mulliken populations, we have also evaluated the Mulliken populations from the GVB(6/PP) wave function for comparison (see Table II).

In the $\bar{\sigma}$ system the polarity of the CH and CN σ leads to a small negative charge (−0.148) on the carbon and a rather large negative charge (−0.372) on the center N. The buildup of charge on the center N in the $\bar{\sigma}$ system is compensated for in the $\bar{\pi}$ system by a movement of charge from the center N onto the C and end N. This leads in the $\bar{\pi}$ system to a negative charge on the C (−0.335) and end N (−0.264) and a large positive charge on the center N (+0.599). In the $\pi_y(\bar{\sigma})$ system the shift of charge toward the end nitrogen occurring in the $\bar{\pi}$ system is compensated for by charge flow from the end N to the center N.

The Mulliken populations are in rough accord with the contributions to dipole moment. However, use of Mulliken

Table II. Mulliken Populations and Net Charges for the Ground State of H_2CNN[a]

	1s	1s′	2s	2s′	x	x′	y	y′	z	z′
					Mulliken Populations					
NA	1.1605	0.8335	0.9131	0.9011	1.0454	0.2895	0.6546	0.1536	0.9749	0.1312
NB	1.1594	0.8346	0.8910	0.4841	1.0062	0.3945	0.9233	0.2974	1.0797	−0.0765
C	1.1739	0.8201	0.7121	0.5254	0.9321	0.3323	0.9676	0.1795	0.7391	0.0305
HA	0.5090	0.2592								
HB	0.5090	0.2592								

	C	NA	NB	HA	HB
		Net Charges[b]			
The π_x system	−0.335	+0.599	−0.264		
The π_y pair		−0.221	+0.192		
The $\bar{\sigma}$ system	−0.148	−0.372	+0.086	+0.232	+0.232

[a] GVB(3/PP). [b] Net charges are relative to (19).

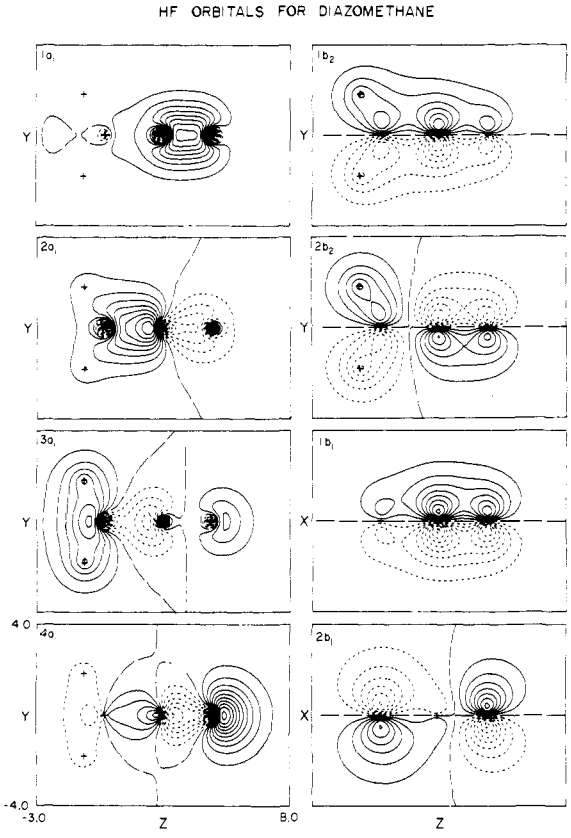

Figure 4. The HF orbitals of the $X(^1A_1)$ state of diazomethane.

Table III. Energies for the Ground State of Diazomethane (Energies in hartrees, Relative to HF)

MBS		DZ	
HF (ref 17)	+0.29687	HF (ref 18)	+0.01328
HF (this work)	+0.00000[a]	HF (this work)	0.00000[b]
GVB(3/PP)	−0.07374	GVB(3/PP)	−0.07844
GVB(6/PP)	−0.09080[c]	GVB(6/PP)	−0.11422
GVB(3)-CI	−0.12651	GVB(3)-CI	−0.12811

[a] −147.30687 hartrees. The other energies in this column are relative to this energy. [b] −147.78348 hartrees. The other energies in this column are relative to this energy. [c] In the MBS GVB(6/PP) wave function we restricted the CH pairs to be symmetry functions. While the description in terms of symmetry functions is equivalent to a localized orbital description at the HF level, at the GVB level the two are not equivalent. For the DZ basis the GVB(6/PP) energy was lower for localized CH orbitals and the same is probably true for MBS.

Table IV. Overlaps and Pair Splittings[a]

	Diazomethane		CH_2[b] and N_2[c]	
Pair	Energy lowering, hartrees	Overlap	Energy lowering, hartrees	Overlap
CH σ left	0.01292	0.8524	0.0139	0.842
CH σ right	0.01292	0.8524	0.0139	0.842
CN σ	0.01098	0.8786		
NN σ	0.01011	0.8946	0.0123	0.8940
π_x GVB pair	0.03838	−0.6023	0.03182	0.6969
π_y GVB pair	0.03593	0.6703	0.03182	0.6969

[a] DZ basis, GVB(6/PP). [b] Reference 5c. [c] T. H. Dunning, Jr., and D. C. Cartwright, to be published.

populations to predict dipole moments would be suspect since the N(2s) term dominating the dipole moment would be ignored.

D. The Hartree–Fock Orbitals. The HF orbitals for the ground state of diazomethane are shown in Figure 4. Comparing with the GVB orbitals of Figure 1 there are only slight resemblances. On the other hand, from (9) and (10) we see that a GVB pair can be reduced to a doubly occupied HF-like pair by merely deleting the second configuration ($\phi_{i2}\phi_{i2}$). This corresponds to just averaging the two GVB orbitals together in order to obtain the HF orbital. Doing this for all six pairs of Figure 1 leads to a Slater determinant of doubly occupied orbitals in (21) with an energy only 0.00696 hartree = 0.189 eV above the self-consistent HF wave function of H_2CNN.

$$\mathcal{A}\{[\phi_{11}\phi_{11}][\phi_{21}\phi_{21}]\ldots\chi\} \qquad (21)$$

However, despite the close correspondence in energies we see that the HF orbitals (Figure 4) are quite different from averages of the GVB orbitals. Averaging the GVB orbitals leads to doubly occupied orbitals corresponding to localized CH bonds, CN σ bonds, NN π bonds, etc., whereas the HF orbitals are much more delocalized.

What is the problem here; why are the HF orbitals so delocalized? Basically, the problem is that the HF orbitals are not unique. With a Slater determinant of doubly occupied orbitals we can take any nonsingular linear transformation among the occupied orbitals without making *any* change in the energy or any property of the molecule. The usual choice of the HF orbitals is to use the eigenfunctions of the HF one-electron Hamiltonian

$$H^{HF}\varphi_i = \epsilon_i\varphi_i$$

$$H^{HF} = h + \sum_i (2J_i - K_i) \qquad (22)$$

which does indeed lead to a unique set of orbitals (ignoring trivial flexibility for degenerate orbitals). Should the particular orbitals obtained from (22) lead to more useful interpretations than the other choices? There is some reason to believe so. In fact, Koopmans showed that the orbitals from (22) are optimally adjusted for describing the *positive ion* (within the restriction that the orbitals of the ground state are unchanged upon ionization). The usual HF MO's, or rather their energies, are indeed quite useful for interpreting the photoelectron spectra of molecules, as would be expected from Koopmans' theorem. However, it does not follow from this that these same orbitals would be particularly useful for understanding the chemical or physical properties of the neutral molecule.

The inappropriateness of the HF canonical orbitals as a basis for chemical concepts of molecules has long been noted and a number of techniques for obtaining more localized forms of the HF orbitals have been suggested. The GVB method provides yet another way of obtaining localized HF orbitals. Essentially, the set of HF-like orbitals obtained from (20) is that combination of the HF orbitals that is optimal for correlating the wave function. Thus viewing each GVB pair as

$$\varphi_a\varphi_b + \varphi_b\varphi_a = C(\varphi_g\varphi_g - \lambda\varphi_u\varphi_u)$$

the set of first natural orbitals spans essentially the same space as is spanned by the HF orbitals and the set of second natural orbitals φ_u provides the correlation effects. Applying the variation principle we find that the correlation correction effects are largest when both φ_g and φ_u are localized in the same region.[16]

E. Energies. Energies for the GVB and HF wave function for the ground state of diazomethane are listed in Table III. Table IV contains some of the special parameters of the GVB(6/PP) wave function. Note that most of the energy lowering in the GVB(6/PP) wave function as compared

Table V. CI Energies for Diazomethane Excited States

State	MBS, eV	DZ basis: Ground state core, eV	DZ basis: SCF core, eV	DZRx basis: Ground state core, eV	DZRx basis: SCF core, eV	Expt,[e] eV
$X(^1A_1)$	0.0[a]	0.0[b]				
$^3A_2$	2.84		2.65[d]			
$^1A_2$	3.23	3.31	2.93[c]			3.14
$^3A_1$	3.68	3.66				
$2(^1A_1)$	7.85	7.39		6.89[c]	5.90[c]	5.70

[a] MBS GVB(3)-CI energy = −147.43338 hartrees. [b] DZ GVB(3)-CI energy = −147.91159 hartrees. [c] Energy relative to DZ GVB(3)-CI. [d] An SCF core appropriate to the singlet state was used. [e] Absorption maximum.

with HF comes from correlation of the $\pi_x(\tilde{\pi})$ and $\pi_y(\tilde{\sigma})$ pairs.

As a test of the perfect pairing assumption we carried out configuration interaction (CI) calculations using the orbitals from the GVB(3/PP) wave function. We find that the GVB-PP wave function contains about two-thirds of the correlation energy in the GVB(3)-CI. The additional energy lowering in the CI was primarily due to $\sigma \rightarrow \sigma^*$ $\pi \rightarrow \pi^*$ double excitations, and we conclude that the perfect pairing restriction had little effect on the shapes of the orbitals. This is generally the case for closed shell systems near the equilibrium geometry.

F. The Separated Limits and the Nature of the Bond. Starting with the GVB wave function for the ground state of diazomethane and pulling off the N_2 along a linear path (C_{2v} symmetry) the lowest limit (about 3.4 eV above the ground state) would be the ground state of $N_2(X^1\Sigma_g^+)$ and the 2^1A_1[19] state of CH_2

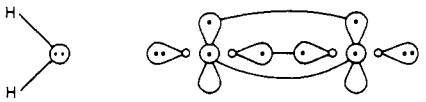

(23)

A higher energy limit (about 7.4 eV above the ground state) would be the ground state of methylene (X^3B_1) and the $^3\Pi$ excited state of N_2

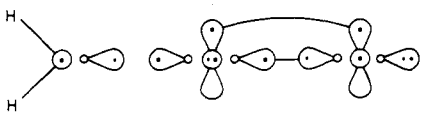

(24)

Although (24) is considerably higher (~4 eV) than (23) the orbitals of the ground state of diazomethane are very similar to (24). In fact, bringing methylene (X^3B_1) up to N_2 ($^3\Pi_g$) as shown so as to form a CN σ bond, we would expect the doubly occupied π_{ux} orbital of N_2 to delocalize somewhat onto the carbon and concomitantly the singly occupied N_2 π_{gx} orbital to localize toward the terminal nitrogen. At the same time, the singly occupied methylene $1b_1$ orbital (π_x) must build in a nodal plane to become orthogonal to the double occupied N_2 π_{ux} orbital. In fact, at the equilibrium geometry the ϕ_c orbital still resembles the π_{ux} orbital of N_2 while the ϕ_l and ϕ_r orbitals resemble the $1b_1$ orbital of CH_2 and the π_{gx} orbital of N_2, respectively. Either limit in (23) or (24) involves a large promotion energy and hence we expect a weak CN bond in diazomethane, as found experimentally and in our calculations.[20,21]

IV. The Excited States

A. The $^3A_2$ and $^1A_2$ States. To find low-lying excited states of diazomethane we will start with (19) and search for other ways of distributing the electrons over the valence orbitals of the atoms without disrupting the σ bonds. Assuming the linear CCN configuration the most favorable case is

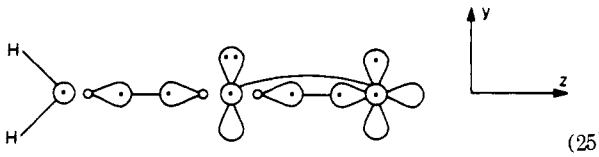

(25)

which leads to $^3A_2$ and $^1A_2$ states. This has the same atomic configuration on each atom and the same number of σ and π bonds. However, in (25) the doubly occupied p_y orbital on the central N cannot delocalize onto the carbon (because of the CH bonds), whereas the corresponding (p_x) orbital of (19) can. As a result the singly occupied p_y orbital on the terminal atom of (25) is much more antibonding than the corresponding (p_x) orbital of (19). In addition, in (19) the singlet state is stabilized by the $\phi_l\phi_r$ pairing, an effect lost in (25) where the singly occupied orbitals are orthogonal. Given these differences it is not surprising that the vertical excitation energies to the $^3A_2$ and $^1A_2$ states are 2.65 and 2.93 eV, respectively (see Table V). Since the singly occupied orbitals are orthogonal, the $^3A_2$ state should be below the $^1A_2$ state and since the singly occupied orbitals are concentrated at opposite ends of the molecule, the exchange integral should be small and hence the triplet–singlet splitting small.

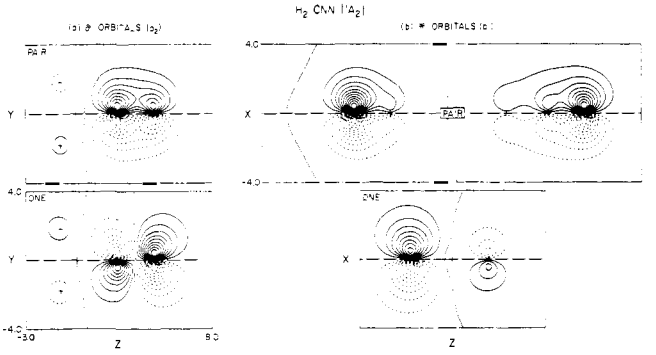

Figure 5. The GVB(3/PP) $\pi_x(\tilde{\pi})$ and $\pi_y(\tilde{\sigma})$ orbitals of the $^1A_2$ state of diazomethane.

In Figure 5 we show the DZ $\tilde{\pi}$ and in-plane π-like ($\tilde{\sigma}$) orbitals of the $^1A_2$ state.

Looking first at the three-electron π_x system, we see that this system corresponds closely to that of allyl radical. However, here one of the resonance structures is far lower in energy than the other. The system is thus well described by a $\tilde{\pi}_x$ pair (with components on the center nitrogen and end nitrogen) and a singly occupied orbital on carbon. Comparing the doubly occupied $N(^2P)\tilde{\sigma}$ orbital on the center nitrogen with (25), we see that it has delocalized strongly toward the end nitrogen concomitantly with the singly occupied 2p $\tilde{\sigma}$ orbital on the end nitrogen building in a nodal plane to remain orthogonal. The decrease in energy associated with the delocalization of the doubly occupied $\tilde{\sigma}$ orbital is thus somewhat offset by the now highly antibonding singly occupied $\tilde{\sigma}$ orbital. In order to decrease these interactions we expect the molecule to bend within the yz plane toward (26). However, the configuration in (26) is

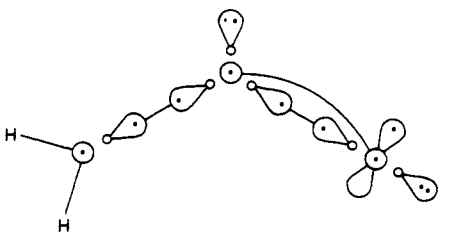

(26)

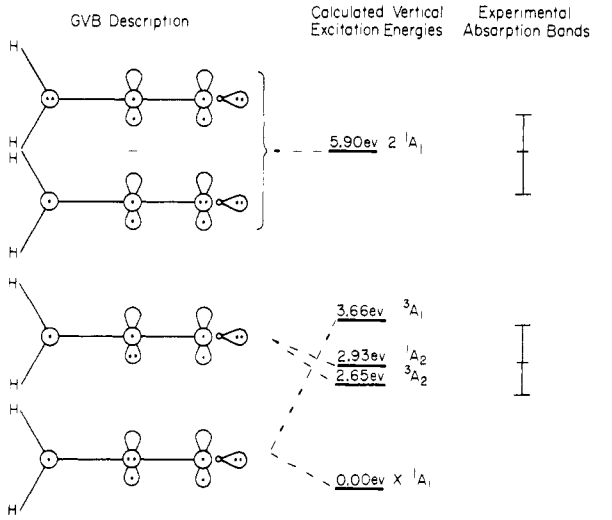

Figure 6. The GVB descriptions of the low-lying states of diazomethane.

compatible with dissociation to

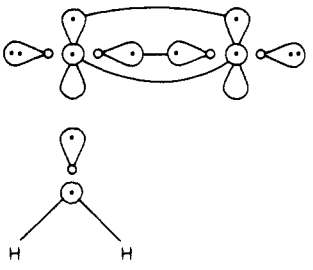

(27)

leading to the formation of $CH_2(^3B_1)$ and $N_2(^1\Sigma_g^+)$. For the $^1A_2$ state, however, the corresponding limit $CH_2(^1B_1)$ and $N_2(^1\Sigma_g^+)$ is 1.9 eV higher. Since the $^1A_1 \rightarrow {}^1A_2$ excitation energy is 2.9 eV and the ground state is bound by ~1.5 eV with respect to $CH_2(^3B_1)$ and $N_2(^1\Sigma_g^+)$, the $^1A''$ state of (25) is bound by ~0.5 eV with respect to products in (26). [Dissociation to $N_2(X^1\Sigma_g^+) + CH_2(^1A_1)$ should be exothermic by ~1 eV.]

Excitation to the $^1A_2$ state is dipole forbidden but vibronically allowed. We identify the $^1A_2$ state with the diffuse weak absorption with maximum at 3.14 eV (see Figure 6).

The delocalization of the π_y orbital on the central N (corresponding to the p pair of the ^2P state) also leads to a large increase in the dipole moment of this state as compared with the ground state (see Table VI). In fact the dipole moment of the $^1A_2$ state is calculated to be +3.62 D [GVB(3)-CI] as compared with the ground state dipole moment of +1.86 D [GVB(3)-CI]. The charge distribution in the $^3A_2$ state is expected to be quite close to that in the singlet state and indeed the dipole moment of the $^3A_2$ state is +3.54 D [GVB(3)-CI]. A detailed breakdown of the dipole moment of the $^1A_2$ state into orbital contributions is given in Table I.

B. The $^3A_1$ State. Starting with the $\bar{\pi}$ orbitals of the X^1A_1 ground state (19) and (20) and coupling the ϕ_l and ϕ_r orbitals antisymmetrically

$$\phi_c^2(\phi_r\phi_l - \phi_l\phi_r) \tag{28}$$

leads to the $^3A_1$ state of H_2CNN. In the simple approximation in which the same orbitals are used for both states, the excitation energy is

$$\Delta E = -A/(1 - S^2) \tag{29}$$

Table VI. Dipole Moments (in Debye) for the Valence States of H_2CN_2[a]

	X^1A_1	$^3A_1$	2^1A_1	$^1A_2$	$^3A_2$
HF	+1.69				
GVB(3/PP)	+1.99			3.11	
GVB(6/PP)	+1.98				
CI	+1.86	2.64	0.21	3.62	3.54
Exptl	±1.50[b]				

[a] All calculations use the DZ basis. A positive dipole moment implies that the terminal nitrogen is negative. [b] Reference 8.

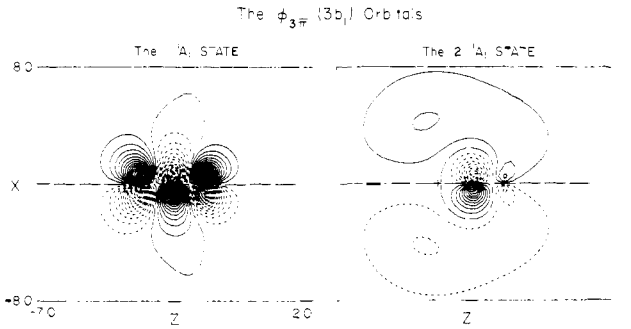

Figure 7. The $3b_1(\pi^*)$ orbitals for the 2^1A_1 and X^1A_1 states. (Contour interval = 0.02 au.)

where A is a (negative) quantity approximately proportional to the square of the overlap, S, of the ϕ_l and ϕ_r orbitals.[22] For ozone $S = -0.28$ and $\delta E = 1.4$ eV, for H_2 molecule $S = 0.80$ and $\Delta E = 10$ eV, and for ethylene $S = 0.64$ and $\Delta E = 4.2$ eV (all vertical excitation energies). Thus for H_2CNN with $S = -0.60$ the calculated $\Delta E = 3.66$ eV is reasonable.

Defining delocalized orbitals (MO's) $\phi_{\overline{2\pi}}$ and $\phi_{\overline{3\pi}}$ as

$$\phi_{\overline{2\pi}} = (\phi_l - \phi_r)/\sqrt{2(1 - S)}$$
$$\phi_{\overline{2\pi}} = (\phi_l + \phi_r)/\sqrt{2(1 + S)} \tag{30}$$

where the constant factors ensure normalization, the $\bar{\pi}$ part of the singlet state (20) becomes

$$\psi_S = \phi_c^2\{(1 - S)\phi_{\overline{2\pi}}\phi_{\overline{2\pi}} - (1 + S)\phi_{\overline{3\pi}}\phi_{\overline{3\pi}}\} \tag{31}$$

while the triplet state (28) becomes

$$\psi_T = \phi_c^2(\phi_{\overline{2\pi}}\phi_{\overline{3\pi}} - \phi_{\overline{3\pi}}\phi_{\overline{2\pi}}) \tag{32}$$

For the self-consistent orbitals of the ground state, S is negative (see Figure 1), hence (31) may be written

$$\psi_S = \phi_c^2(a_{\overline{2\pi}}\phi_{\overline{2\pi}} - b\phi_{\overline{3\pi}}\phi_{\overline{3\pi}}) \tag{33}$$

where for the self-consistent wave function a is 0.9705 and b is 0.2410. The MO description of the singlet state has the form (33) except that the $\phi_{\overline{3\pi}}\,\phi_{\overline{3\pi}}$ term is deleted, while the MO description of the triplet state is (32). Thus, in the MO description the $^3A_1 \leftarrow {}^1A_1$ transition is described as $3\bar{\pi} \leftarrow 2\bar{\pi}$ and these states appear to be quite different [The MO excitation energy will be low by 1.044 eV (the π_x splitting energy) because the triplet state is correctly described, while for the singlet state the second configuration $\phi_{\overline{3\pi}}\,\phi_{\overline{3\pi}}$ is neglected.] On the other hand, the GVB wave functions [(20) and (28)] for the two states involve similar orbitals and differ mainly in the way in which the orbitals are coupled. We thus expect somewhat similar charge distributions in the two states and in fact the calculated dipole moment of the $^3A_1$ state is 2.64 D [GVB(3)-CI], a value not drastically different from the dipole moment of the ground state.

Table VII. CH_2N_2 Rydberg States

IVO symmetry	IVO character	State symmetry	IVO excitation energy, eV	Quantum defect δ	Oscillator strength	Expt, eV	Assignment
a_1	3s	$^1B_1$	5.89	0.905	5.4×10^{-3}		Not observed
a_1	3p	$^1B_1$	6.87	0.467	3.2×10^{-3}	6.51	1900 Å group
a_1	3d	$^1B_1$	7.48	−0.001	3.8×10^{-3}		
b_1	3p	$^1A_1$	6.91	0.443	1.2×10^{-1}	5.70	2^1A_1 state
b_1	3d	$^1A_1$	7.68	−0.222	5.7×10^{-3}	7.37	(First member of d Rydberg series)
b_1	4p	$^1A_1$	8.24	−0.258	9.7×10^{-2}		
b_2	3p	$^1A_2$	6.65	0.589	0.0	6.51	1900 Å group
b_2	3d	$^1A_2$	7.59	−0.117	0.0		

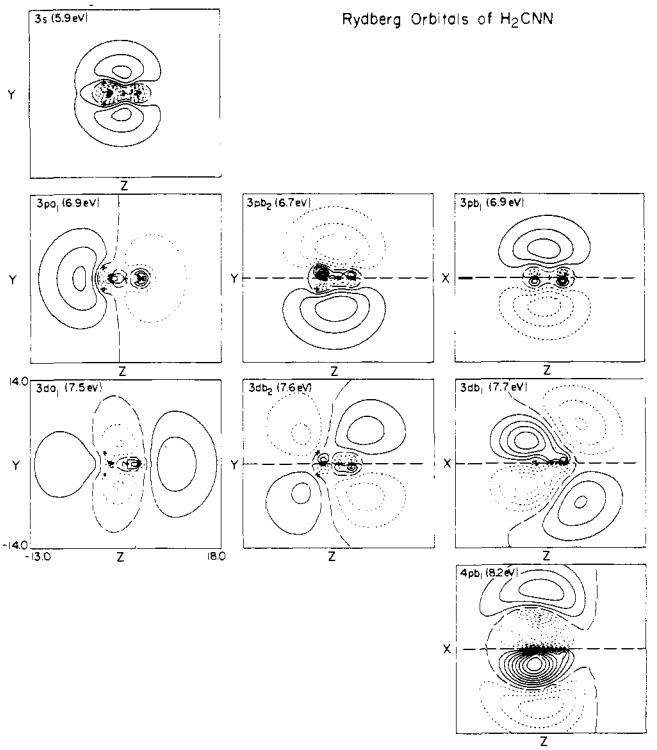

Figure 8. The Rydberg orbitals. (Contour interval = 0.01 au.)

C. The 2^1A_1 State. Given the MO wave function 32 one can obtain a new singlet state (2^1A_1)

$$\phi_C{}^2(\phi_{\overline{2\pi}}\phi_{\overline{3\pi}} + \phi_{\overline{3\pi}}\phi_{\overline{2\pi}}) \tag{34}$$

with the same configuration. However, within the approximation that $\phi_{\overline{2\pi}}$ and $\phi_{\overline{3\pi}}$ be described with (30), (34) is equivalent to the wave function

$$\phi_C{}^2[\phi_l\phi_l - \phi_r\phi_r] \tag{35}$$

which corresponds approximately to the zwitterion structures I and II that are often used to describe the ground state.

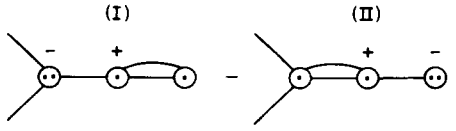

(36)

While we did not solve for the orbitals of (34) in a fully self-consistent calculation (it is the second CI root of A_1 symmetry), we did carry out a pseudo-SCF calculation in which the $\phi_{\overline{2\pi}}$ orbital is frozen. Doing this we find that the resulting $\phi_{\overline{3\pi}}$ orbital becomes diffuse (Rydberg-like). This behavior is analogous to that of the corresponding $\pi \rightarrow \pi^*$ singlet state of ethylene.[23]

However, the form of the wave function 35 is dependent on the specific choices for the orbital expansion coefficients in (30). While (30) was appropriate to the ground state and $^3A_1$ state, the actual $\phi_{\overline{3\pi}}$ orbital of the 2^1A_1 state (Figure 7) is more concentrated on C; thus, a more reasonable approximation to this orbital would be

$$\phi_{\overline{3\pi}} \cong \phi_l' \tag{37}$$

(where ϕ_l' is a diffuse atomic 3p orbital on C). Choosing for the other two orbitals the π_x orbitals appropriate to the positive ion state

$$\phi_{\overline{1\pi}} \cong \phi_l$$
$$\phi_{\overline{2\pi}} \cong \phi_c + \phi_r \tag{38}$$

leads to the wave function

$$(\phi_c + \phi_r)^2(\phi_l'\phi_l + \phi_l\phi_l') \tag{39}$$

which is essentially I of (36).

Thus, the 2^1A_1 state may be regarded as a charge transfer state resulting from excitation of an electron from the ϕ_r component of the π_x GVB pair into the ϕ_l component of the pair I. Since the doubly occupied orbital is shifted toward the terminal N, the structure II that would result from exciting the ϕ_l component of the GVB π_x pair into the ϕ_r component is higher in energy and the wave function is mostly I. Given this description, one expects the 2^1A_1 state to have a smaller dipole moment than the ground state. Indeed, the calculated dipole moment [GVB(3)-CI using a ground state σ core] is 0.21 D.

Excitation to the 2^1A_1 state from the ground state is expected to be strong. [The calculated oscillator strength for the $2^1A_1 \leftarrow X^1A_1$ transition is 0.376.] Our CI calculations place the 2^1A_1 state at 5.90 eV (vertical) and we identify it with the observed strong absorption peaked at 5.70 eV. Structure I is expected to be repulsive because of bad pair–pair interactions between the (essentially) N_2 doubly occupied π_x orbital and the doubly occupied CH_2 $1b_1$ orbital (as in He_2). The $^1\Sigma_g^+$ state of methylene (linear) is about 2.5 eV above the $^1A_1$ state; thus assuming that bending the $CH_2(^1\Sigma_g^+)$ state does not markedly increase the energy, and using the experimental $D(H_2C{-}N_2) = 1.8$ eV, it seems energetically feasible for the $2(^1A_1)$ state to dissociate directly to $CH_2(2^1A_1)$ and $N_2(X^1\Sigma_g^+)$. Indeed retaining C_{2v} symmetry, the system is essentially forced to go to this set of limits. This conclusion is in line with the observation by Herzberg that flash excitation of CH_2N_2 using light of 210 nm leads to excited singlet states of methylene as the primary products.[24] Of course the reaction can also proceed through bent geometries leading to the production of methylene in lower states.

D. Rydberg States. In the above sections we discussed the low-lying excited states expected to arise from excitations among the valence orbitals. Other low-lying excited states are expected to correspond to excitation into diffuse Rydberg-like orbitals. To examine such states diffuse basis functions were added to our basis (see section IB). Rather than solving self-consistently for each excited state, we used the IVO approach of Hunt and Goddard[25] in which the correct variational Hamiltonian for the excited orbital is set up and diagonalized over the orbitals orthogonal to the occupied orbitals of the ground state. Thus, with one diagonalization, one gets all excited orbitals (out of a particular ground state orbital and for a particular total spin).

The calculated excitation energies[25b] and oscillator strengths are given in Table VII and plots of the Rydberg orbitals are given in Figure 8.

The Orbitals. The assignment and calculated energy of each Rydberg orbital is given in Figure 8.

As expected the three 3p orbitals have similar energies as do the three 3d orbitals solved for. There is a 0.9 eV separation between the 3s and 3p states and a 0.8 eV separation between the 3p and 3d states, reasonable results given the different abilities of these orbitals to penetrate the H_2CNN^+ core.

Looking more closely we see that the 3s orbital is squished away from the CH bonds and N lone pair, apparently due to repulsive effects with these pairs. This change in shape can be described as subtraction of d_{z^2} character $(2z^2 - x^2 - y^2)$ from the 3s wave function.

The $3pb_2$ orbital corresponds closely to the shape expected for a 3p orbital. The $3pa_1$ orbital deviates somewhat, concentrating more on the H_2C end of the molecule. This is apparently in response to the shift of the σ system to the right making the N end less attractive for the Rydberg state.

The $3pb_1$ orbital corresponds closely to the shape expected for a 3p orbital. However, there are complications here. This orbital leads to the second A_1 state of H_2CNN, discussed in section IVC. Carrying out a CI calculation leads to the introduction of valence character in the wave function and a decrease in the energy of this state to 5.9 eV.

Since diffuse s and p functions were placed on each atom, we expect a good description of the 3s and 3p Rydberg states. Although diffuse d functions were not included we expect moderately good descriptions of the the $3d_{z^2}$, $3d_{xz}$, and $3d_{yz}$ excited orbitals from combining the diffuse function on various centers. A much poorer description of 4s, 4p, and higher states is expected since sufficiently diffuse functions were not included.

The 3d orbitals being the highest of the $n = 3$ orbitals are distorted in the unfavorable directions (e.g., toward the end N). The exception is $3db_1$, which has a large amount of carbon valence character.

The Energies. Rydberg states are often characterized in terms of a quantum defect, δ defined as

$$\text{IP(hartrees)} = 1/2(n - \delta)^2 \qquad (40)$$

in terms of the ionization potential of the excited state (in hartrees). Thus, δ is the correction to the principle quantum number that would lead to an energy expression like that of the hydrogen atom.

The calculated quantum defects are listed in Table V. The average values $\delta_{3s} = 0.905$, $\delta_{3p} = 0.500$, and $\delta_{3d} = -0.113$ are all a bit smaller than for smaller molecules, indicating extra repulsive interactions due to the core.

The calculated excitation energy into the 3s orbital ($^1B_1$ state) is 5.89 eV. However, the calculated oscillator strength is 5.4×10^{-3} and this transition is probably buried under the strong absorption due to the 2^1A_1 state (calculated $f \approx 0.376$).

At shorter wavelengths, Merer[26] has observed an extensive series of perpendicular bands near 1900 Å (6.51 eV). At 1585 Å (7.65 eV) there is a similar series of perpendicular bands. Herzberg[27] has pointed out that these two-band systems fit reasonably well as the first two members of an np series with $\delta = 0.67$ leading to an IP of 9.06 eV.

Our calculations show a $^1B_1$ state at 6.87 eV and also a $^1A_2$ state at 6.65 eV corresponding to excitation to $3pa_1$ and $3pb_2$ orbitals, respectively. However, Merer's analysis of the 1900 Å group indicated three very closely spaced states, two of B_1 symmetry and a third which did not seem to have "any intensity of its own in absorption" (which Merer tentatively assigned as a B_2 state). It seems reasonable that our $^1B_1$ state is one of Merer's B_1 states. The $^1A_2$ state is not dipole allowed but becomes vibronically allowed for B_1, B_2, and A_2 vibrations. We suggest that the remaining states analyzed by Merer (B_1 and B_2) may correspond to vibronically induced transitions $^1A_2 \leftarrow X^1A_1$.

Since we did not include sufficiently diffuse basis functions to describe 4p orbitals, our results cannot be used to verify the assignment of the 1585 Å group to 4p Rydberg levels.

We find three states of 3d character near 7.6 eV. Without d functions explicitly in our basis we may expect to be a bit high on these states (as evidenced by negative quantum defects) and hence it appears reasonable to associate the $^1A_1$ 3d Rydberg state with the first member of the parallel nd Rydberg series observed by Herzberg (7.37 eV). To obtain a good description of these Rydberg levels d functions should be included, a calculation we intend to pursue later.

V. Details of the CI Calculations

While the GVB(6/PP) wave function for the ground state of diazomethane is highly useful for interpretation purposes, it is clear from Table IV that the major part of the ground state correlation energy is contained within a two-pair wave function in which the π_x and π_y pairs are split. For our CI studies we have used the orbitals of GVB(3/PP) wave functions in which the π_x, π_y, and CN σ pairs are split.

In all the CI calculations the three 1s-like orbitals were kept doubly occupied (this allows these electrons to be eliminated from all calculations by appropriately modifying the one-electron integrals). For the MBS-CI calculations there are 14 additional basis functions for describing 11 occupied GVB orbitals. For each state we started with the dominant configuration for that state and included all single and double excitations among the 11 GVB orbitals.

For the DZ and DZRx bases we carried out self-consistent GVB(3/PP) calculations for the X^1A_1, 1^1A_2, and 2^1A_1 states. These self-consistent vectors were then used in the corresponding CI calculations (for the $^3A_1$ state we used X^1A_1 vectors and for $^3A_2$ we used $^1A_2$ vectors). In each case the doubly occupied σ orbitals of the GVB(3/PP) calculations were kept paired in the CI. Based on the results from MBS-CI, we also made the following restriction in the CI. The orbitals for the CI were partitioned into subspaces corresponding to a_1, b_1, and b_2 symmetries, respectively, and only excitations within these symmetry types were allowed. Within this restriction all single and double excitations were taken from the appropriate dominant configurations. This procedure leads to a significant reduction in the number of configurations while allowing a good description of the excitation energies.

We also solved for the various states using the GVB vectors of the ground state. In these calculations we included

configurations involving single excitations from the π GVB orbitals into the remaining π virtuals (a procedure referred to as polarization CI). This latter calculation leads to errors for the excited $^1A_2$ and 2^1A_1 states of 0.4 to 1.5 eV which can be attributed to two effects: (1) lack of relaxation of the unexcited orbitals and (2) a restricted description of the excited orbital. Probably (2) is the most important for $^1A_2$ but core relaxation is responsible for lowering the excitation energy of 2^1A_1 by about 1 eV (for the DZRx basis). This large effect is due to the diffuse nature of the excited orbital of the 2^1A_1 state, leading to significant contraction of the other orbitals upon excitation.

A. The $^1A_2$ and $^3A_2$ CI Calculations. We used the $^1A_2$ DZ GVB(2) orbitals as a basis for π-electron CI calculations on the $^1A_2$ and $^3A_2$ states. We also carried out polarization CI calculations using the GVB(3) ground state orbitals.

B. The $^3A_1$ and 2^1A_1 CI Calculations. The $^3A_1$ and 2^1A_1 states both arise from the π_x electron configuration.

$$1b_1{}^2 2b_1 3b_1 \tag{41}$$

However, as has been previously shown (sections IVB and IVC), the $^3A_1$ state corresponds basically to the triplet coupling of the GVB π_x pair, whereas the 2^1A_1 state is a charge transfer state. Thus, the $^3A_1$ state should be well described with orbitals much like the ground state GVB π_x natural orbitals, whereas we expect the 2^1A_1 state to have a diffuse $3b_1$ orbital in agreement with the ionic character of the state.

We carried out π electron polarization CI calculations on the $^3A_1$ state using the DZ GVB(3) natural orbitals as a basis. From an examination of the single excitations, it is clear that the DZ basis is adequate to describe this state and that the π_x orbitals are not much different from those for the singlet state.

For the 2^1A_1 state we used the configurations for polarization CI plus additional configurations from allowing all double excitations within the b_1 space. Using the DZ GVB(3) orbitals and the above configurations, we find a sizable improvement over the MBS results. Examination of the single excitations indicates that the variationally correct $3b_1$ orbital would have large amplitudes on the more diffuse p_x basis functions. Augmenting the basis with a single diffuse p_x function on each center (DZRx) and repeating the CI with a similar set of configurations resulted in another decrease in the energy, with the $3b_1$ orbital again showing large amplitudes on the most diffuse functions. However, this calculation still used a frozen σ core appropriate to the ground state. In order to obtain a more contracted σ core appropriate to the diffuse $3b_1$ orbital, we carried out CI calculations using the GVB(3/PP) vectors from the pseudo-SCF calculation described in section IVC. The $3b_1$ orbital from this calculation was found to have large amplitudes on the most diffuse p_x basis functions and to have a small orbital energy (−0.077111 hartree) consistent with a Rydberg-like orbital. Using the σ core from this calculation in a π electron CI calculation on the 2^1A_1 state and using the same spatial configurations as in the previous CI with ground state core an energy only 0.2 eV above the experimental λ_{max} was obtained.

Examining the CI results for the 2^1A_1 state, we see that the best CI energy (DZRx, SCF core) is a full 2.0 eV below the MBS CI, whereas for the other states the MBS CI gave excitation energies essentially the same as were obtained with the more extensive DZ basis. This is, of course, strong evidence for the ionic character of the 2^1A_1 state. It is interesting to note that 1.0 eV of the difference between our final CI result for the 2^1A_1 state and the MBS result is due to a σ core contraction in response to excitation into a diffuse $3b_1$ orbital.

VI. Ground State Chemistry of Diazomethane

Diazomethane belongs to a class of compounds commonly referred to as 1,3 dipoles because the principal resonance structures drawn to describe the bonding are zwitterion structures. For example for diazomethane these structures are

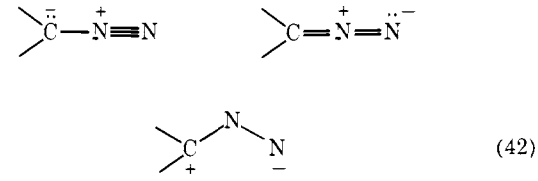

(42)

However, we find that the ground state is more accurately described as biradical-like, although, as discussed earlier, there is a fairly large overlap between the $\phi_l\phi_r$ components of the π_x GVB pair.

Roberts[28] has pointed out that the GVB description yields a simple consistent rationalization of the facile 1,3 addition of diazomethane to olefins. Usually the dipolar nature of diazomethane
is considered as the dominant influence. However, abundant experimental evidence suggests that this reaction occurs in a one-step process not involving charge separation.[29]

On the other hand, the GVB model of diazomethane suggests a biradical attack analogous to that in ozone. In particular we note that cycloaddition of diazomethane to ethylene does preserve orbital phase continuity.[30] This follows from the fact that the overlap between the $\phi_l\phi_r$ components of the GVB π_x pair results from a through-bond coupling rather than a direct coupling as for ethylene. Thus, to get a positive S_{lr} the orbitals must be oriented as in (43).

(43)

Therefore, the phases are preserved in the cycloaddition, so that the reaction is expected to be concerted.

Addition of Methylene to N_2. Recently several investigators have observed recombination of $CH_2(^1A_1)$ and $N_2(^1\Sigma_g{}^+)$ to give diazomethane. Moore and Pimentel[31] have observed recombination of N_2 and methylene in an N_2 matrix at liquid He temperatures. In line with this observation, Bass et al.[32] have had to postulate reaction between methylene singlet and N_2 to explain their kinetic studies of N_2/CH_2N_2 mixtures following flash excitation. Based on the rate constant for the N_2-methylene recombination derived by Bass et al., Laufer and Okabe[21] estimate an activation energy of ≤ 3 kcal/mol. Moore and Pimentel conclude that recombination of CH_2 and N_2 to give diazirine has a much higher activation energy, since they do not observe diazirine formation. In fact, they show that formation of diazomethane in diazirine photolysis is a result of recombination of CH_2 (produced in the diazirine photolysis) with matrix N_2.

The formation of diazomethane with a small activation energy and the failure to observe diazirine in the reaction between $CH_2(^1A_1)$ and $N_2(X^1\Sigma_g{}^+)$ may be understood using the orbital phase continuity principle and concepts from the GVB description of diazomethane.

Consider the following reaction path 44. For this orientation closure to the symmetric diazirine is not favored. However, using large θ (>120°) leads to orbitals with the same

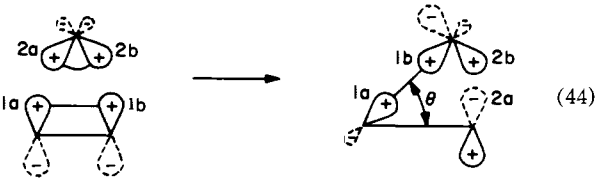

(44)

phase orientation as in (43), thus we expect the energy to decrease monatomically as the molecule opens to diazomethane and hence a predominance of diazomethane, as is observed.

References and Notes

(1) Partially supported by a grant (GP-40783X) from the National Science Foundation.
(2) National Defense Education Act Fellow.
(3) For an interesting example and further references, see J. E. Bercaw, E. Rosenberg, and J. D. Roberts, *J. Am. Chem. Soc.*, **96**, 612 (1974).
(4) See D. J. Cram and G. S. Hammond, "Organic Chemistry", McGraw-Hill, New York, N.Y., 1964.
(5) (a) W. A. Goddard III, T. H. Dunning, Jr., W. J. Hunt, and P. J. Hay, *Acc. Chem. Res.*, **6**, 368 (1973); (b) W. J. Hunt, P. J. Hay, and W. A. Goddard III, *J. Chem. Phys.*, **57**, 738 (1972); (c) P. J. Hay, W. J. Hunt, and W. A. Goddard III, *J. Am. Chem. Soc.*, **94**, 8293 (1972); (d) A. P. Mortola and W. A. Goddard, *ibid.*, **96**, 1 (1974).
(6) As an example, consider a four-electron singlet. There are two possible spin couplings: $\chi_1 = 0.5(\alpha\beta - \beta\alpha)(\alpha\beta - \beta\alpha)$ and $\chi_2 = (3^{1/2}/6)[2(\alpha\alpha\beta\beta - \beta\beta\alpha\alpha) - (\alpha\beta + \beta\alpha)(\alpha\beta + \beta\alpha)]$. We may define a general spin eigenfunction (SEF) by $\chi = \cos\theta\chi_1 + \sin\theta\chi_2$ and then solve for the spin coupling simultaneously with obtaining the optimum orbitals.
(7) In many cases solving for χ as above results in only the χ_1 coupling being important, $\chi = (\alpha\beta - \beta\alpha)(\alpha\beta - \beta\alpha) \ldots (\alpha\beta - \beta\alpha)$. When we force χ to have this form, the wave function is denoted by PP for "perfect pairing". We may then write our GVB wave function as $\mathcal{A}\{\varphi_{1a}\varphi_{1b}\varphi_{2a}\varphi_{2b} \ldots \varphi_{na}\varphi_{nb}\}\chi_{PP}$, which is equivalent to $\mathcal{A}\{[(\varphi_{1a}\varphi_{1b} + \varphi_{1b}\varphi_{1a})(\varphi_{2a}\varphi_{2b} + \varphi_{2b}\varphi_{2a}) \ldots](\alpha\beta\alpha\beta \ldots \alpha\beta)\}$.
(8) A. P. Cox, L. F. Thomas, and J. Sheridan, *Nature (London)*, 181, 1000 (1958); J. Sheridan, *Adv. Mol. Spectrosc., Proc. Int. Meet., 4th 1959*, **1**, 139 (1962).
(9) (a) S. Huzinaga, D. McWilliams, and B. Domsky, *J. Chem. Phys.*, **54**, 2283 (1972); (b) T. H. Dunning, Jr., *ibid.*, **53**, 2823, (1970).
(10) (a) See F. W. Bobrowicz, Ph.D. Thesis, California Institute of Technology, March 1974. (b) Written by F. W. Bobrowicz (vide supra) and N. W. Winter utilizing spin eigenfunction techniques of R. C. Ladner (see Ph.D. Thesis, California Institute of Technology, November 1971). Modifications due to L. A. Harding, S. P. Walch, B. J. Moss, and W. A. Goddard III.
(11) Taking our wave function for the N(^{4}S) state as $\psi = \mathcal{A}(\varphi_{sz}\varphi_{\bar{s}z} + \varphi_{\bar{s}z}\varphi_{sz})2p_x2p_y2p_z\alpha\beta\alpha\alpha$, where $\varphi_{sz} = \varphi_{2s} + \lambda\varphi_{2p_z}$ and $\varphi_{\bar{s}z} = \varphi_{2s} - \lambda\varphi_{2p_z}$, we see that this is equivalent to $\mathcal{A}[\varphi_{2s}^2 - \lambda\varphi_{2p_z}^2)2p_x2p_y2p_z\alpha\beta\alpha\alpha]$, which reduces to $\mathcal{A}[\varphi_{2s}^2 2p_x2p_y2p_z\alpha\beta\alpha\alpha]$ due to the antisymmetrizer.
(12) L. Harding and W. A. Goddard III, *J. Am. Chem. Soc.*, in press.
(13) F. Grimaldi, A. Lecourt, and C. Moser, *Int. J. Quantum Chem.*, **15**, 153 (1967).
(14) S. Green, *Chem. Phys. Lett.*, **23**, 115 (1973).
(15) S. P. Walch and W. A. Goddard III, *Chem. Phys. Lett.*, **33**, 18 (1975).
(16) The energy change due to the $\phi_u\phi_u$ configuration is approximately $\Delta E = -(K_{gu})^2/(E_u - E_g)$, and thus the correlation effected by ϕ_u favors maximizing K_{gu}. To maximize K_{gu}, one needs to concentrate ϕ_g and ϕ_u both in the same regions of space.
(17) J.-M. Andrè, M. Cl. Andrè, G. Leroy, and J. Weiler, *Int. J. Quantum Chem.*, **3**, 1013 (1969).
(18) L. Snyder and H. Basch, "Molecular Wave Functions and Properties Tabulated from SCF Calculations in a Gaussian Basis Set", Wiley, New York, N.Y., 1972.
(19) This corresponds to the $^1\Sigma_g^+$ state of linear CH_2 or to the MO occupancy $1a_1^2 2a_1^2 2b_2^2 1b_1^2$ of bent CH_2.
(20) Using the GVB(3/PP) energy of $CH_2(^1A_1)$ (ref 5c) and estimating the GVB(3/PP) energy of N_2 by adding the pair lowerings for each pair (Table IV) to the HF energy (ref 9b) leads to an H_2C–N_2 bond energy of 0.88 eV for diazomethane in the DZ basis. The best experimental estimate (ref 21) of this quantity is 2.31 eV. Since we did not include d functions in the basis, errors of the order of 1 eV are expected in bond dissociation energies, approximately the value obtained.
(21) A. H. Laufer and H. Okabe, *J. Am. Chem. Soc.*, **93**, 4137 (1971). We use their value relative to $^3B_1$ methylene and add 0.50 eV as the $^1A_1 \leftarrow {}^3B_1$ excitation energy for methylene (ref 5c).
(22) (a) C. W. Wilson, Jr., and W. A. Goddard III, *Theor. Chem. Acta*, **26**, 195 (1972); (b) W. A. Goddard III and C. W. Wilson, Jr., *ibid.*, **26**, 211 (1972); (c) C. W. Wilson, Jr., and W. A. Goddard III, *Chem. Phys. Lett.* **5**, 45 (1970).
(23) T. H. Dunning, Jr., W. J. Hunt, and W. A. Goddard III, *Chem. Phys. Lett.*, **4**, 147 (1969).
(24) G. Herzberg, *Proc. R. Soc. London, Ser. A*, **262**, 291 (1961).
(25) (a) W. J. Hunt and W. A. Goddard III, *Chem. Phys. Lett.*, **3**, 414 (1969); see also W. J. Hunt, Ph.D. Thesis, California Institute of Technology, September 1971. (b) In the IVO procedure it is the ionization potential (IP) of the excited (Rydberg) orbital that is calculated. To obtain excitation energies, this is subtracted from the experimental IP, 8.99 eV for H_2CNN.
(26) A. J. Merer, *Can. J. Phys.*, **42**, 1242 (1964).
(27) G. Herzberg, "Electronic Spectra and Electronic Structure of Polyatomic Molecules", Van Nostrand-Reinhold, New York, N.Y., 1966.
(28) J. D. Roberts, private communication.
(29) R. Huisgen, *Angew. Chem.*, **2**, 633 (1963).
(30) W. A. Goddard III, *J. Am. Chem. Soc.*, **94**, 793 (1972).
(31) C. B. Moore and G. C. Pimentel, *J. Chem. Phys.*, **41**, 3504 (1964).
(32) W. Braun, A. M. Bass, and M. Pilling, *J. Chem. Phys.*, **52**, 5131 (1970).

Molecular Orbital Theory of the Hydrogen Bond. XIII. Pyridine and Pyrazine as Proton Acceptors

Janet E. Del Bene

Contribution from the Department of Chemistry, Youngstown State University, Youngstown, Ohio 44555.

Received January 29, 1975

Abstract: Ab initio SCF calculations with a minimal STO-3G basis set have been performed to determine the equilibrium structures and energies of dimers HF–pyrazine, HF–pyridine, and H_2O–pyridine. The structures of the equilibrium dimers are consistent with structures anticipated from the general hybridization model. The HF–pyridine dimer is more stable than the HF–pyrazine dimer. Its greater stability may be attributed to the presence of a more negatively charged nitrogen atom in pyridine, and to a favorable alignment of molecular dipole moments in the HF–pyridine dimer. An HF–pyridine dimer in which hydrogen bond formation occurs through the π electron system at the nitrogen has also been investigated and found to be a nonequilibrium structure on the intermolecular surface. CI calculations have been performed to determine $n \rightarrow \pi^*$ transition energies for the monomers pyrazine and pyridine, the equilibrium dimers, and a 2:1 HF–pyrazine trimer. The results suggest that when pyridine is the proton acceptor molecule, the hydrogen bond is broken upon excitation in the dimer, but when pyrazine is the proton acceptor, the hydrogen-bonded complex remains bound in the excited $n \rightarrow \pi^*$ state.

In many chemical and biochemical systems, the aromatic nitrogen atom is an important proton acceptor atom for hydrogen bond formation. It is of interest, therefore, to extend ab initio molecular orbital studies of hydrogen bonding to include dimers in which an aromatic compound is the proton acceptor molecule, with hydrogen bond formation occurring through a lone pair of electrons on a nitrogen atom. While molecular orbital calculations on dimers with proton acceptor nitrogens have previously been reported, the proton acceptor molecules in these dimers have generally been